# Liquefaction analysis of unsaturated ground affected by earthquake with long-term strong ground motion duration

Takaki Matsumaru[1], T. Sato[1], and R. Uzuoka[2]

[1] Structures Technology Division, Railway Technical Research Institute, 2-8-38, Hikari-cho, Kokubunji, Tokyo 185-8540, Japan.
[2] Disaster Prevention Research Institute, Kyoto University, Gokasho, Uji, Kyoto 611-0011, Japan.

## ABSTRACT

In this paper, the numerical analysis focused on the liquefaction of unsaturated ground was performed with the three-phase (soil, water, and air) coupled analysis based on porous media theory. In this technique, the conventional constitutive model for describing the cyclic behavior of unsaturated soil was employed. From the numerical simulations about the shaking table test of unsaturated ground, it was revealed that the simulation could reproduce the experimental results well. Furthermore, the series of simulations indicated that the long-term strong ground motion caused liquefaction widely and severely in unsaturated region and the seismic behavior of the ground was also affected.

**Keywords:** liquefaction; unsaturated ground; seismic response analysis; long-term strong motion duration

## 1 INTRODUCTION

It was reported that liquefaction occurred even in unsaturated ground in the past earthquake. In order to evaluate the mechanism of this behavior, experimental and numerical studies have been conducted widely recently. However, the influence of the duration of the ground motion on liquefaction in unsaturated ground has not been made clear.

In this paper, the liquefaction analyses were performed in order to clarify this influence on the occurrence of liquefaction of unsaturated ground. As the numerical simulation method, the three-phase (soil, water, and air) coupled analysis based on porous media theory was adopted. For the constitutive model for soil skeleton, the simplified cyclic elasto-plastic model considering the effect of the suction was applied.

First, the numerical simulation of the shaking table tests of unsaturated ground was conducted in order to obtain the applicability of the method for the prediction of liquefaction of unsaturated ground. The increase of the pore water pressure and the response acceleration in the unsaturated region were examined. Furthermore, the numerical simulations of unsaturated ground were conducted. In these analyses, the influence of the duration time of strong motion and the initial distributions of degree of saturation were examined.

## 2 NUMERICAL METHOD

In this study, the governing equations for three phase mixture (soil particle, pore water, and pore air) were adopted (Uzuoka and Borja, 2012). The governing equations were formulated based on the following assumptions:

1) The conditions are isothermal;
2) The soil particles are incompressible;
3) The mass exchange among phases can be neglected;
4) The material time derivative of relative velocities and the advection terms of pore fluids to the soil skeleton can be neglected.

The governing equations consist of the momentum balance equations of mixtures and the mass and momentum balance equations of pore water and air.

The weak forms were implemented in finite element formulation. The Newmark implicit scheme is used for time integration. The primary variables are the second-order material time derivatives of the displacement of soil skeleton, pore water pressure and air pressure. The weak forms are linearized and solved by the Newton-Raphson method iteratively at each time step. In the finite element formulation, Galerkin method and isoparametric 8-node elements are used. The soil skeleton displacement and the fluid pressures are approximated at 8 nodes and 4 nodes respectively to satisfy the discrete LBB conditions.

For the constitutive equation for liquefiable sand, a cyclic elasto-plastic model (Matsumaru and Uzuoka, 2014) was applied. This constitutive model was formulated on the following assumptions:

1) The infinitesimal strain theory;
2) The elasto-plastic theory;
3) The non-associated flow rule and the Cam-clay type plastic potential function;
4) The non-linear kinematic hardening rule (Armstrong and Fredrick 1966) and the dependency of hardening parameters on the amount of plastic

strain.

## 3 NUMERICAL SIMLATION OF SHAKING TABLE TEST OF UNSATURATED GROUND

### 3.1 Outline of shaking table test

Fig. 1 shows the experimental model of the 1-g shaking table test of the unsaturated ground with the finite element model. The water level was located at the height of 60 cm from the bottom of the liquefiable layer, and the surface layer with 30 cm of thickness was in unsaturated condition.

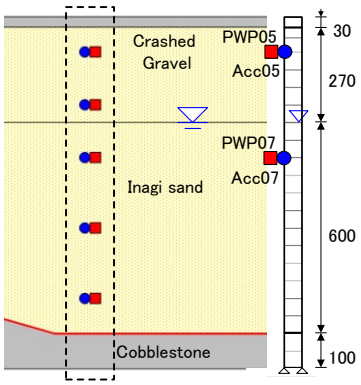


Fig. 1. Experimental and analytical model.

The material of the ground was Inagi sand, whose particle density $G_s$ was 2.723; 50% diameter on the grain size diagram $D_{50}$, 0.134mm; the uniformity coefficient $U_c$, 9.29; the fine fraction content $F_c$, 23.6 %; and the maximum dry density, 1.517 g/cm$^3$. The liquefiable ground was prepared so that the dry density and the water content would be 1.108 g/cm$^3$ and about 13% respectively. The water level was located at the height of 70 cm from the bottom of the liquefiable layer, so the surface layer with 30 cm of thickness was in unsaturated condition. At the surface of the ground, the crashed gravel was prepared for modeling the subgrade of rail track. At the bottom, cobblestone was prepared in order to make the ground in saturated condition easily.

Fig. 2 shows the time history of the input motion. The sinusoidal wave with 3 Hz was used. The amplitude was 100 gal initially and changed to 200 gal after 70 second. The duration time was about 170 seconds.

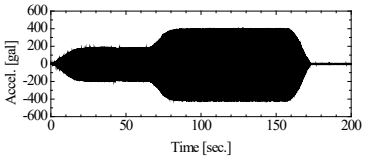


Fig. 2. Time history of inputted motion.

### 3.2 Analytical conditions

In numerical simulation, the 1-dimensional column model was prepared as shown in Fig. 1. Before conducting the seismic response analysis, the initial stress condition was calculated by static weight analysis. In the seismic response analysis, the dissipation boundary for pore water was prepared at the surface of the ground. This means that dissipation occurred when the pore ware pressure changed to zero.

The elasto-plastic constitutive model was applied for the liquefiable sand layer. For the soil water characteristic curve, the logistic function model (Sugii et al, 2002) was used. The series of the unsaturated cyclic triaxial tests were conducted in initial different values of suctions, and the model with successfully reproduced the tendency of the increase of the pore water and air pressure and the decrease of the mean skeleton stress (Matsumaru and Uzuoka 2014).

### 3.3 Results and discussions

Fig. 3 shows the time histories of the excess pore water pressures (EPWP; increment of the pore water pressure after starting the shaking) and the response accelerations. PWP07 and Acc07 were located under the water level, and PWP05 and Acc05 were located in the unsaturated region. In the experiment, the excess pore water pressure at PWP07 increased at first. The excess pore water pressure at PWP05 also increased after the increase of PWP05. It seems that the increase of the excess pore water pressure in the unsaturated region was caused by the increase of the pore water pressure at the saturated region and the seepage of pore water from the saturated region. The numerical simulations successfully reproduced well the time and the amount of the increase of the pore water pressure.

The decrease of the response acceleration occurred at about 40 seconds. Though the time when the acceleration decreased in the simulation was a little bit earlier, the simulation successfully reproduced the tendency of the response acceleration obtained in the experiment. After the occurrence of the decrease of the acceleration, the amplitude at A05 was smaller than that at A07. The increase of the excess pore water pressure occurred even in the unsaturated region, so the response at the surface would become smaller.

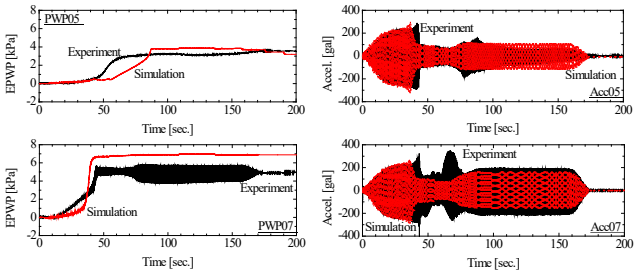


Fig. 3. Time histories of excess pore water pressure and response acceleration.

## 4 EFFECT OF LONG TERM STRONG MOTION TO LIQUEFACTION OF UNSATURATED GROUND

### 4.1 Analytical conditions

Fig. 4 shows the analytical model. The dimension of model was 13 m in depth and the water level was located at 3 m. The elements e1 to e12 were liquefiable layer and the elements e1 to e6 were also liquefiable even in unsaturated conditions.

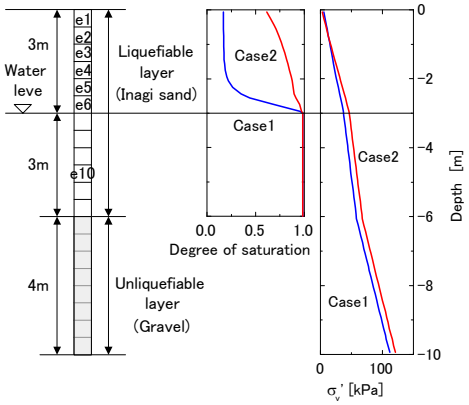


Fig. 4. Analytical model.

Fig. 5 shows the time histories of the seismic motion. For the input acceleration, two motions "Kobe wave" and "Mito wave" were prepared. Kobe wave was observed at the depth of GL-16m at Port-Island in the 1995 Hyogo-ken Nambu earthquake, 1995. Mito wave was based on the wave of EW component recorded at K-NET Mito in the 2011 off the Pacific coast of Tohoku earthquake. Though the maximum amplitudes for both motions were about 570 gal, the duration time for Mito wave was ten times longer than that for Kobe wave.

For the analytical cases, the different initial distributions of degree of saturations were considered. For both cases, the seismic response analysis was conducted by use of two motions as shown in Fig. 5. In Case 1, the degree of saturation was close to the residual value above the water level. In Case 2, the degree of saturation was larger than Case 1 and the value at the surface was about 60 %. In Fig.4, the distributions of the initial vertical skeleton stress were plotted for both cases. From this figure, the initial values of degree of saturation were largely different among cases. Due to the differences of the suction and the degree of saturation in the unsaturated region, the vertical skeleton stress in Case 1 was smaller about 10 kPa than that in Case 2, under the water level.

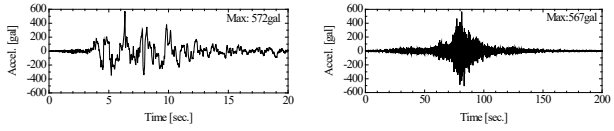


Fig. 5. Time histories of input accelerations.

### 4.2 Results and discussions

Fig. 6 shows the time histories of pore water pressure for both cases and both analyses using different input motions. The time histories contain the behaviors of the elements in the unsaturated region (e1 to e6). In the analyses using Kobe wave, only the pore water pressure at e6 located just above the water level increase and the others were maintained at the initial value. On the other hand, in the analyses using Mito wave, the increase of the pore water pressure occurred at e5 and e6 in Case 1 and at e2 to e6 in Case 2. Especially, the pore water pressures changed from negative to positive value in Case 2. Due to the long-term strong ground motion, the region where the pore water pressure increased was enlarged in unsaturated region.

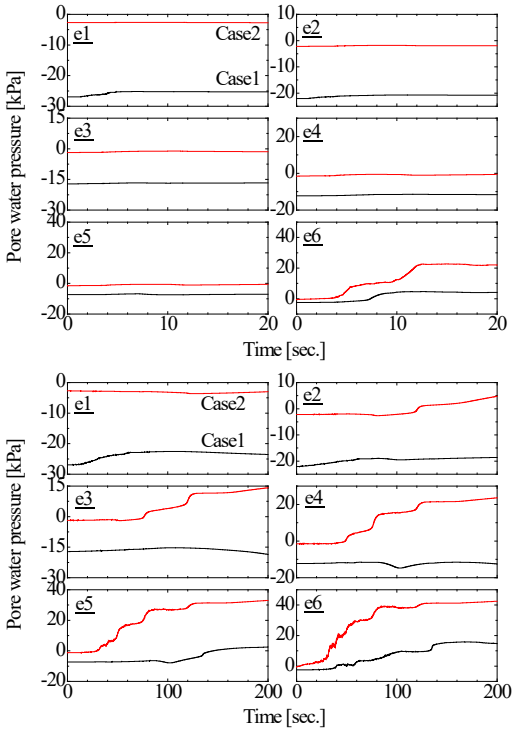


Fig. 6. Time histories of pore water pressure.

Fig. 7 shows the changes of the distributions of mean skeleton stress reduction ratio (MSSRR) for using both waves in Case 2. This figure contains the distributions at 10 and 20 seconds for Kobe wave and at 50, 100, 150 and 200 seconds for Mito wave. In the analysis using Kobe wave, the increase of MSSRR was observed only at e6 just above the water level and its value was about 0.4. So, the initial stress condition was maintained in unsaturated region. On the other hand, in the analysis using Mito wave, the region where MSSRR increased was enlarged from the element e6 to the upper elements during the earthquake. Because the pore water pressure easily increased due to the influence of the long-term strong ground motion as shown in Fig. 6, the region where MSSRR increased was enlarged.

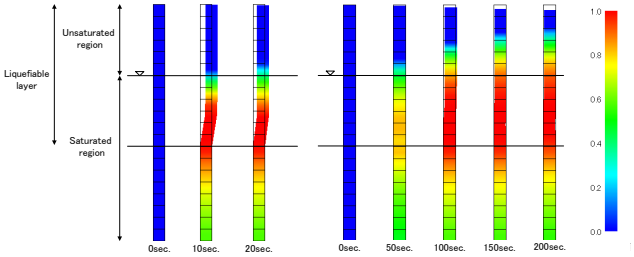


Fig. 7. Distributions of mean skeleton stress reduction ratio.

Fig.8 shows the time histories of vertical displacement at the surface of the ground. In the analyses using Kobe wave, the displacements in two cases were mostly the same. However, in the analyses using Mito wave, the difference of the displacements between two cases appeared at about 100 seconds and the residual settlement in Case 1 was 1.5 times larger than that in Case 2. At 100 seconds, the pore water pressure largely increased as shown in Fig. 6 and the large increase of MSSRR was observed at e5 and e6 as shown in Fig. 7. The degree of the occurrence of liquefaction in unsaturated region would cause the difference of the displacement between two cases.

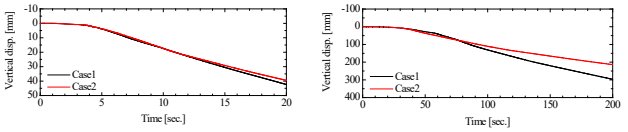


Fig. 8. Time histories of vertical displacement at surface of ground.

In order to clarify the reason of the difference of the displacements between two cases for the analyses using Mito wave, Fig. 9 shows the relationship between vertical strain $\varepsilon_y$ and shear stress $\sigma'_{xy}$ at e6 and e10. The element e10 is located in saturated region. At e10, the shear stress caused by earthquake decreased and the vertical strain increased due to the decrease of the stiffness. The increase of the vertical strain in Case 1 was larger than that in Case 2. On the other hand, the strain e6 in Case 2 was smaller than that in Case 1. However, the vertical strain mainly increased in saturated region, so the settlement in Case 1 became larger than that in Case 2.

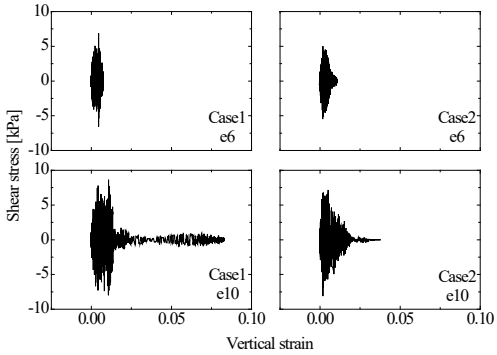


Fig. 9. Relationship between vertical strain and shear strain.

Fig. 10 shows comparisons of the horizontal response acceleration at the surface of the ground in the analyses using Mito wave. The response accelerations were largely different between two cases. The difference appeared at about 40 seconds, when the increase of the pore water pressure in unsaturated region started. The degree of the occurrence of the liquefaction in unsaturated region caused the difference of the seismic behavior.

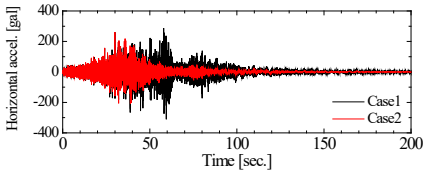


Fig. 10. Time histories of horizontal response acceleration.

## 5 CONCLUSIONS

In this paper, the liquefaction analysis was performed in order to clarify this influence on the occurrence of liquefaction of unsaturated ground. As a result, the following conclusions were obtained.

1. Numerical analyses could reproduce well the increase of the pore water pressure and the response acceleration in unsaturated ground compared with the results obtained in the shaking table test.
2. Due to the effect of the long-term duration motion, the amount and the region of the increase of the pore water pressure became larger. Furthermore, it was revealed that the seismic behavior was also affected by the degree of the liquefaction in unsaturated region.

## ACKNOWLEDGEMENTS

The authors would like to express their appreciation to the National Research Institute for Earth Science and Disaster Prevention for allowing the use of their K-NET record in this paper.

## REFERENCES

Uzuoka, R. and Borja R.I. (2012). Dynamics of unsaturated poroelastic solids at finite strain, International Journal for Numerical and Analytical Methods in Geomechanics, 36, 1535-1573.

Matsumaru, T. and Uzuoka, R. (2014). Three-phase coupled analysis of unsaturated embankment subjected to rainfall infiltration and seismic motion, Unsaturated Soils: Research & Applications, 597-604.

Armstrong, P. J. and Frederick. C.O. (1966). A mathematical representation of the multiaxial Bauschinger effect, Technical report C.E.G.B.Report RD/B/N731, Berkeley Nuclear Laboratories.

Sugii, T., Yamada, K. and Kondou, T. (2002). Relationship between soil-water characteristic curve and void ratio, Proceedings of 3rd International Conference of Unsaturated Soils, 209-214.